The thickness of the turbulent/nonturbulent interface is equal to the radius of the large vorticity structures near the edge of the shear layer

Carlos B. da Silva[a] and Rodrigo R. Taveira
IDMEC/IST, Technical University of Lisbon, Pav. Mecânica I, 1º Andar, Av. Rovisco Pais, 1049-001 Lisboa, Portugal

(Received 14 August 2010; accepted 24 November 2010; published online 21 December 2010)

Direct numerical simulations at Reynolds numbers ranging from $\mathrm{Re}_\lambda = 30$ to 160 show that the thickness δ_ω of the turbulent/nonturbulent (T/NT) interface in planar jets is of the order of the Taylor scale $\delta_\omega \sim \lambda$, while in shear free, irrotational/isotropic turbulence is of the order of the Kolmogorov microscale $\delta_\omega \sim \eta$. It is shown that δ_ω is equal to the radius of the large vorticity structures (LVSs) in this region, $\delta_\omega \approx R_{\mathrm{LVS}}$. Thus, the mean shear and the Reynolds number affect the T/NT interface thickness insofar as they define the radial dimension of the LVS near the T/NT interface. © *2010 American Institute of Physics*. [doi:10.1063/1.3527548]

Free shear flows e.g. jets are divided into two regions: in one region, the flow is turbulent (T), while in the other region, the flow consists of irrotational [or nonturbulent (NT)] flow.[1] The two regions are separated by a sharp interface—the turbulent/nonturbulent (T/NT) interface—which is continually deformed over a wide range of scales.[2] Turbulent entrainment is the mechanism by which fluid elements from the irrotational flow region acquire turbulence, and become part of the turbulent region, and governs the exchanges of mass, momentum, and scalar quantities across the T/NT interface. Contrary to the classical view that turbulent entrainment is governed by large-scale "engulfing," recent works suggest that it is mainly caused by small-scale "nibbling".[3,4]

A longstanding issue in this context is the existence of a viscous superlayer[1] where a viscous process is responsible for the spreading of vorticity from the turbulent into the irrotational flow region. Indeed, until now, observation of this viscous superlayer has been elusive.[5] A related problem concerns the thickness of the T/NT interface δ_ω, which can be seen as the inner layer of the viscous superlayer.[4,5] The T/NT interface is characterized by a sharp rise in the vorticity magnitude across a very thin region.[2,4,6–8] Defining δ_ω as the thickness associated with this vorticity jump, it has been noticed that the observed values for δ_ω vary in literature between $\eta < \delta_\omega < \lambda$, where η and λ are the Kolmogorov and Taylor microscales, respectively; e.g., in the experimental results from round jets[4,5] and in direct numerical simulation (DNS) of plane jets,[7,8] $\delta_\omega \sim \lambda$, whereas in a turbulent front generated from an oscillating grid, $\delta_\omega \sim \eta$.[6]

The goal of the present work is to study the influence of the Reynolds number and mean shear on the thickness of the T/NT interface δ_ω. For this purpose, several DNSs were carried out using (i) planar turbulent jets (PJETs) and (ii) shear free irrotational/isotropic turbulence (SFIIT). Table I lists the physical and computational parameters of all the simulations used here. The planar turbulent jet uses the numerical algorithm described in Refs. 7 and 9, employing pseudospectral methods for spatial discretization and a three-step third order Runge–Kutta scheme for temporal advancement. The reference simulation—PJET_{120}—is described in Ref. 7. The self-similar regime is obtained at $T/T_{\mathrm{ref}} \approx 20$, where $T_{\mathrm{ref}} = H/(2U_1)$ and U_1 and H are the initial velocity and the jet slot width, respectively; the Reynolds number based on the Taylor microscale λ and on the root-mean-square of the streamwise velocity u' is $\mathrm{Re}_\lambda = u'\lambda/\nu \approx 120$. The other jet simulations, e.g. PJET_{160}, are essentially similar to PJET_{120} but were carried out at different Reynolds numbers. The effect of the initial conditions is tested with the simulation $\mathrm{PJET}_{\mathrm{chan}}$ where the initial condition consists of interpolated velocity fields from a DNS of a turbulent channel flow,[10] while the other jet simulations use a "spectral" synthetic noise superimposed to a hyperbolic tangent mean velocity profile as in many other DNSs of jets.[11]

In order to study the effect of the mean shear on δ_ω, we carry out DNSs of SFIIT with the same code used for the planar jet. In these simulations, an irrotational/isotropic turbulence boundary is generated by instantaneously inserting a velocity field from a previously run DNS of (forced) isotropic turbulence into the middle of a field of zero initial velocity. As time progresses, the initial isotropic turbulence region spreads into the irrotational region in the absence of mean shear. The imposition of these initial boundary conditions can be easily accomplished by drastically reducing the time step in the simulations when the boundary condition is inserted, as described in Ref. 12 where similar simulations were reported. The simulations SFIIT_{30} and SFIIT_{110} differ essentially in the Reynolds number and resolution. In the irrotational region and far away from the T/NT interface $\langle u'^2 \rangle \sim y_I^{-4}$ for both simulations, where y_I is the distance from the T/NT interface, as predicted in Ref. 13.

It is instructive to see the coherent vortices that exist near the T/NT interface in all three major configurations studied here: plane jet started from a synthetic noise, plane jet started from a fully developed turbulent channel flow, and shear free layer separating isotropic turbulence from an irrotational field. Figure 1 shows the isosurfaces of low pressure and positive Q, where Q is the second invariant of the velocity gradient tensor for simulations PJET_{120}, $\mathrm{PJET}_{\mathrm{chan}}$, and

[a]Electronic mail: carlos.silva@ist.utl.pt.

TABLE I. Simulations analyzed in the present study: plane jet (PJET) and shear free irrotational/isotropic turbulence (SFIIT). $PJET_{120}$ is the simulation used in Refs. 7 and 9. $N_x \times N_y \times N_z$ is the number of colocation points along the streamwise (x), normal (y), and spanwise (z) directions and $L_x \times L_y \times L_z$ is the size of the computational domain. T^* is the time interval from which the data were used for analysis. For PJET, $T^* = T/T_{\mathrm{ref}}$, while for SFIIT, $T^* = 2\sqrt{\nu T}/\lambda$. δ_ω is the thickness of the T/NT interface and R_{LVS} is the estimated radius of the bigger LVS.

Simulation	Re_λ	$N_x \times N_y \times N_z$	$L_x \times L_y \times L_z$	Initial cond.	T^*	$\frac{\delta_\omega}{H}$	$\frac{\delta_\omega}{\eta}$	$\frac{\delta_\omega}{\lambda}$	$\frac{R_{\mathrm{LVS}}}{\lambda}$
$PJET_{60}$	60	$256 \times 384 \times 256$	$4H \times 6H \times 4H$	Sint. noise	25–29	0.23	7.4	0.54	0.56
$PJET_{80}$	80	$256 \times 384 \times 256$	$4H \times 6H \times 4H$	Sint. noise	20–25	0.16	8.3	0.41	0.43
$PJET_{100}$	100	$256 \times 384 \times 256$	$4H \times 6H \times 4H$	Sint. noise	16–24	0.16	11.9	0.62	0.58
$PJET_{120}$	120	$256 \times 384 \times 256$	$4H \times 6H \times 4H$	Sint. noise	20–27	0.15	20.5	0.89	0.86
$PJET_{160}$	160	$512 \times 768 \times 512$	$4H \times 6H \times 4H$	Sint. noise	24–26	0.13	34.3	1.34	1.35
$PJET_{\mathrm{chan}}$	110	$384 \times 486 \times 384$	$6.3H \times 6H \times 4.2H$	DNS channel	17–27	0.07	9.7	0.57	0.45
$SFIIT_{30}$	30	$512 \times 512 \times 512$	$2\pi \times 2\pi \times 2\pi$	DNS isotropic	0.2	⋯	2.7	0.34	⋯
$SFIIT_{110}$	110	$256 \times 256 \times 256$	$2\pi \times 2\pi \times 2\pi$	DNS isotropic	0.2	⋯	5.3	0.26	⋯

$SFIIT_{110}$. The coherent structures from the simulated jets [Figs. 1(a) and 1(b)] are similar to many previous DNSs of turbulent plane jets:[11] they can be divided into two classes: intense vorticity structures (IVSs) and large vorticity structures (LVSs). The IVSs are detected through isosurfaces of $Q > 0$ and correspond to structures with particularly intense vorticity, e.g., in Ref. 14, the IVSs are defined as structures with the highest enstrophy that is contained in 1% of the total volume. The IVSs do not show a particular spatial orientation and are similar to the "worms" observed in isotropic turbulence.[14] On the other hand, the LVSs—identified using low pressure isosurfaces—consist of all the remaining (less intense) vorticity structures and exhibit a bigger mean radius and a distinct spatial orientation. The LVSs consist of the big rollers and streamwise vortices that are known to exist in turbulent plane jets. The rollers can be seen as remnants of the Kelvin–Helmholtz vortices generated during the transition to turbulence in the jet. There is, of course, some spatial overlap between the LVSs and the IVSs since the IVSs are extreme events of LVSs. The vortex core radius of these structures R_{LVS} was estimated "manually" by measuring the distance between two opposite maximum tangential velocity peaks caused by the presence of the LVS, where the local velocity at the center of the eddy was removed from the velocity field. For each simulation, a number of LVSs at the edge of the shear layer were used (between 8 and 16 vortices, e.g., 8 vortices for $PJET_{160}$), and the estimated radius R_{LVS} consists of the averaged radius from these vortices. The rms of the radius computed using this procedure varies between $14.5\% < \sqrt{\langle R'^2_{\mathrm{LVS}} \rangle}/\langle R_{\mathrm{LVS}} \rangle < 16.4\%$ (e.g., 14.5% for $PJET_{160}$). A section from the (x,y) plane was used since in a planar jet the bigger vortices tend to be aligned with the azimuthal (z) direction. The streamwise vortices originate in the secondary instabilities and tend to be smaller, with smaller lifetimes [see Figs. 1(a) and 1(b)]. Figure 2(a) illustrates the procedure for one LVS from $PJET_{120}$. In this case, R_{LVS} is of the order of the Taylor microscale $R_{\mathrm{LVS}} \sim \lambda$. The estimated values of R_{LVS} are given in Table I.

Finally, the coherent vortices from shear free turbulence [Fig. 1(c)] are somehow different. Indeed, the LVSs do not really exist in this flow since the absence of a mean shear precludes their formation and only "wormlike" structures are discernible. The procedure outlined above was not used to compute the radius of these structures due to their very small size (of the order of the grid size). However, it is well established[14] that the radius of the worms is $R_{\mathrm{IVS}} \approx 3-5\,\eta$.

As in several previous works,[2,4] we use conditional statistics in relation to the distance from the T/NT interface, denoted by $\langle\ \rangle_I$. This procedure was already described in detail in Ref. 9. The sketch in Fig. 2(b) shows the T/NT interface separating the turbulent from the irrotational flow re-

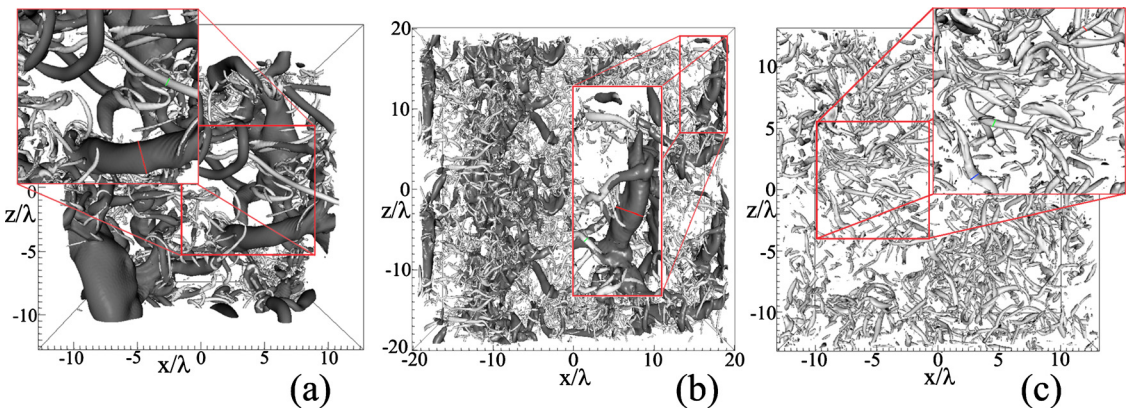

FIG. 1. (Color online) The LVSs and IVSs near the T/NT interface in the PJET and SFIIT. The LVSs are identified through low pressure isosurfaces (dark), while the IVSs are identified through isosurfaces of $Q > 0$ (grey): (a) $PJET_{120}$, (b) $PJET_{\mathrm{chan}}$, and (c) $SFIIT_{110}$.

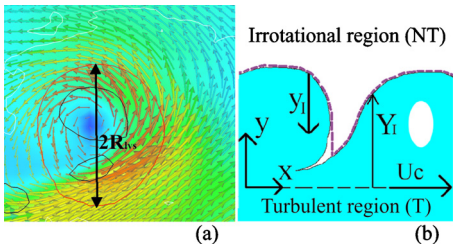

FIG. 2. (Color online) (a) Determination of the radius of the LVS near the jet edge for simulation $PJET_{120}$: $R_{LVS}/\lambda \sim 0.86$. (b) Sketch of the T/NT interface, indicating the vorticity surface (solid line) and the interface envelope (gray dashed lines), with the coordinate system of the plane jet (x,y) and the one used in the conditional statistics in relation to the distance from the T/NT interface (y_I). The interface envelope position is denoted by Y_I.

gions at the upper shear layer of the jet. The T/NT interface is defined by the surface where the vorticity norm $\Omega = (\Omega_i \Omega_i)^{1/2}$ is equal to a certain threshold $\Omega = \Omega_{tr}$, where the particular value of this threshold is obtained as in Refs. 2 and 3. For the planar jet, the detection threshold is $\Omega_{tr} = 0.7 U_1/H$, while for the shear free turbulence, we obtained $\Omega_{tr} = 20\omega'$, where ω' is the mean fluctuating vorticity norm. A new local coordinate system (y_I) is defined at the interface location and the conditional statistics are made in this local coordinate system. The T/NT interface is located at $y_I = 0$, while the irrotational and turbulent regions are defined by $y_I < 0$ and $y_I > 0$, respectively.

Figures 3(a) and 3(b) show conditional mean profiles of $\langle |\Omega_z| \rangle_I$ normalized by the value inside the turbulent region. The distance from the T/NT interface y_I is normalized by the Kolmogorov microscale [Fig. 3(a)] and by the Taylor microscale [Fig. 3(b)]. The vorticity $\langle |\Omega_z| \rangle_I$ exhibits a sharp jump near the T/NT interface for all the simulations used in the present work. This jump "ends" inside the turbulent region by a characteristic $\langle |\Omega_z| \rangle_I$ vorticity "bump," which is also observed in the experimental data from jets in Ref. 4. In the reference simulation—$PJET_{120}$—this maximum occurs at $y_I/\eta \approx 20$, which corresponds to $y_I/\lambda \approx 1$. The thickness of the T/NT interface can be defined by the distance between the T/NT interface $(y_I = 0)$ and the distance where the maximum vorticity inside the turbulent region occurs. With this definition, the thickness of the T/NT interface for the reference simulation $(PJET_{120})$ is equal to $\delta_\omega \sim \lambda$, which is the same value observed in the experimental data for jets.[4] Figures 3(a) and 3(b) show that δ_ω lies roughly between the Kolmogorov and the Taylor microscales $\eta < \delta_\omega < \lambda$ for all the simulations used here, which agrees also with all the known results from the literature.

The influence of the Reynolds number in δ_ω for the plane jet can be assessed by comparing the reference simulation $PJET_{120}$ with similar jet simulations at several Reynolds numbers (see Table I): $PJET_{60}$, $PJET_{80}$, $PJET_{100}$, and $PJET_{160}$. The results show that increasing the Reynolds number, the absolute value of δ_ω decreases; however, the thickness of the T/NT interface remains $\delta_\omega \sim \lambda$ for all three jet simulations using the same initial conditions.

In order to assess the influence of the initial conditions on the plane jet, another simulation was carried out—$PJET_{chan}$—using as initial condition a fully developed turbulent channel flow.[10] For this simulation, the thickness of the T/NT interface is slightly smaller than in the reference simulation with $\delta_\omega \sim 10\eta$ or $\delta_\omega \sim 0.6\lambda$. Notice that the two simulations have a similar Reynolds number, which implies that the observed differences in δ_ω must be explained by the details of the turbulent flow field in the two simulations. One difference lies in the topology of the coherent vortices near the T/NT interface. The visualizations in Figs. 1(a) and 1(b) show that the LVSs near the T/NT interface for $PJET_{chan}$ are smaller and more fragmented than in $PJET_{120}$.

Finally, in order to assess the effect of the mean shear, two simulations of shear free isotropic/irrotational turbulence were used: $SFIIT_{30}$ and $SFIIT_{110}$ (see Table I). For these simulations, δ_ω is roughly equal to $\delta_\omega \sim 3-5\eta$, evidencing a small dependence on the Reynolds number. Interestingly, this value is very close to the observed thickness in the experimental T/NT interface generated from an oscillating grid[6] (without mean shear).

In summary, regardless of the Reynolds number, the thickness of the T/NT interface in a jet is $\delta_\omega \sim \lambda$. For similar initial conditions, jets with smaller Reynolds number tend to have slightly higher values of δ_ω, while for similar Reynolds numbers, jets developing after a typical transition to turbulence exhibit slightly higher values of δ_ω compared to jets that originate from a fully developed turbulent flow (where the LVSs are smaller and more fragmented). Finally, in a shear free layer where the vortices near the T/NT interface are essentially the well known worms from isotropic turbulence, we get $\delta_\omega \sim 3-5\eta$.

Here, we argue that the T/NT interface consists of (or is made up of) LVSs sitting at that location. Specifically, the T/NT interface is the physical line defined by the borders of the LVS in the plane jet and to the IVS in shear free turbu-

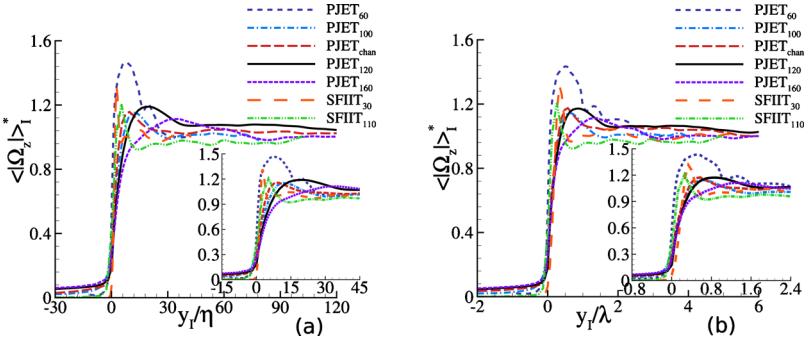

FIG. 3. (Color online) Conditional vorticity profiles $\langle |\Omega_z| \rangle_I$ normalized by the vorticity inside the turbulent region for all the simulations listed in Table I: (a) distance from the T/NT interface in Kolmogorov microscale units—y_I/η; (b) distance from the T/NT interface in Taylor microscale units—y_I/λ. The insets highlight the region near the T/NT interface. Note that η and λ correspond to the values inside the turbulent region ($PJET_{80}$ is not shown for clarity).

lence. The results support this idea since the radius of the larger vortices in each simulation is, in fact, very close to the T/NT interface thickness: in the plane jet $\delta_\omega \approx R_{\mathrm{LVS}}$, whereas in shear free turbulence $\delta_\omega \approx R_{\mathrm{IVS}}$.

The T/NT interface is "made up" both of vorticity from the eddies near the T/NT interface and also of some "incoherent" vorticity that is shed by the vortices as they travel into the T/NT interface. However, the lifetime of this "incoherent vorticity" is small compared to the lifetime of the coherent vortices. Moreover, in a jet, the bigger vortices from the LVS have longer lifetimes than the other LVS or the IVS and therefore have more chance to influence the mean T/NT interface thickness. Specifically, the radial length scale of these structures, i.e., the vortex core sizes should be used since the T/NT interface exhibits a very contorted shape where its surface is formed around the vortices—indeed, defined by the radial size of the vortices—in its proximity. This agrees with the classical picture of the T/NT interface that has been known for some time:[2] the LVSs are responsible for the observed convolutions of the T/NT interface and this explains why the length scale of these convolutions is roughly equal to the radial length scale of the LVS.

The radii of the LVS and IVS near the T/NT interface can be estimated bearing in mind that long lived vortices are vortices where the time-scale associated with the radial viscous diffusion of vorticity is roughly balanced by the axial stretching caused by the local strain rate field S', as in a Burgers vortex,[14] leading to $R \sim (\nu/S')^{1/2}$, where R is the vortex core radius. In a shear layer, it can be argued that the magnitude of the strain rate acting on a LVS near the jet edge is $S' \sim u'/L_{11}$, where u' is the fluctuating velocity field and L_{11} is the integral scale of turbulence.[15] Using the Reynolds number associated with the integral scale $\mathrm{Re}_0 = u' L_{11}/\nu$, the length scale associated with the vorticity jump caused by the vortices is then equal to $\delta_\omega \approx R_{\mathrm{LVS}} \sim \sqrt{\nu/(u'/L_{11})} = L_{11}\,\mathrm{Re}_0^{-1/2} \sim \lambda$. The recent work by Ruban and Vonatsos[16] comes to mind where it is shown that the thickness of a jet front propagating into a quiescent fluid is $O(\mathrm{Re}_0^{-1/2})$. On the other hand, in a shear free flow, as in the flow generated by an oscillating grid,[6] the coherent vortices should be similar to the worms observed in the simulations of isotropic turbulence, where the strain rate acting on the vortices originates in the background turbulence field and is equal to $S' \sim u'/\lambda$. Therefore, the associated length scale of the vorticity jump, i.e., the scale of the vortices near the T/NT interface, is $\delta_\omega \approx R_{\mathrm{IVS}} \sim \sqrt{\nu/(u'/\lambda)} = \lambda\,\mathrm{Re}_\lambda^{-1/2} \sim \eta$, where $\mathrm{Re}_\lambda = u'\lambda/\nu$ is the Reynolds number based on the Taylor microscale. Thus, the problem of determining the thickness of the T/NT interface δ_ω becomes the problem of estimating the radius R of the biggest vortices existing near the edge of the T/NT interface.

Arguably, in the far field of a very high Reynolds number free shear flow, the LVSs tend to be more fragmented and δ_ω may approach the radius of the IVS, $\delta_\omega \sim \eta$. However, there are well documented situations where even at the far field of a very high Reynolds number shear layer the LVSs are still preserved in the flow, and, in this case, we would expect to still have $\delta_\omega \sim \lambda$. Finally, notice that as stressed by an anonymous referee, in some jets the radius of the LVS is of the order of the jet width $R_{\mathrm{LVS}} \sim H$. This situations tends to be more common in the early stages of the transition or in low Reynolds number jet configurations since the initial Kelvin–Helmholtz vortices are less fragmented. PJET_{60} approaches this situation with $\delta_\omega \approx 0.23H$.

Due to the well known computational limitations in DNS, the range of Re_λ used here is necessarily limited. Using $\eta/\lambda \sim \mathrm{Re}_\lambda^{-1/2}$, we can estimate $\Delta(\eta/\lambda)$ for the jet case, giving $\Delta(\eta/\lambda) \sim 44\%$ (between $\mathrm{Re}_\lambda = 60$–160). The observed agreement between δ_ω and R_{LVS} shows the robustness of the present result for this range of Reynolds numbers, which is representative of many fully developed turbulent jets. Assessment of very high Reynolds number flows should be pursued in future works.

In summary, we showed using DNS of planar jets and shear free turbulence at Reynolds numbers ranging from $30 < \mathrm{Re}_\lambda < 160$ that the thickness of the T/NT interface δ_ω at the edge of shear or shear free layers is roughly equal to the size of the largest coherent vortices found at that location and is $\eta < \delta_\omega < \lambda$. The Reynolds number and the magnitude of the mean shear affect the T/NT interface thickness insofar as they define the radial dimension of the large vorticity structures near the interface.

Professor Javier Jiménez is acknowledged for interesting discussions on the definition of the T/NT interface.

[1] S. Corrsin and A. L. Kistler, "Free-stream boundaries of turbulent flows," NACA Technical Report No. TN-1244, 1955.
[2] D. K. Bisset, J. C. R. Hunt, and M. M. Rogers, "The turbulent/non-turbulent interface bounding a far wake," J. Fluid Mech. **451**, 383 (2002).
[3] J. Mathew and A. Basu, "Some characteristics of entrainment at a cylindrical turbulent boundary," Phys. Fluids **14**, 2065 (2002).
[4] J. Westerweel, C. Fukushima, J. M. Pedersen, and J. C. R. Hunt, "Mechanics of the turbulent-nonturbulent interface of a jet," Phys. Rev. Lett. **95**, 174501 (2005).
[5] J. Westerweel, C. Fukushima, J. M. Pedersen, and J. C. R. Hunt, "Momentum and scalar transport at the turbulent/non-turbulent interface of a jet," J. Fluid Mech. **631**, 199 (2009).
[6] M. Holzner, A. Liberzon, N. Nikitin, W. Kinzelbach, and A. Tsinober, "Small-scale aspects of flows in proximity of the turbulent/nonturbulent interface," Phys. Fluids **19**, 071702 (2007).
[7] C. B. da Silva and J. C. F. Pereira, "Invariants of the velocity-gradient, rate-of-strain, and rate-of-rotation tensors across the turbulent/nonturbulent interface in jets," Phys. Fluids **20**, 055101 (2008).
[8] C. B. da Silva and J. C. F. Pereira, "Erratum: 'Invariants of the velocity-gradient, rate-of-strain, and rate-of-rotation tensors across the turbulent/nonturbulent interface in jets' [Phys. Fluids 20, 055101 (2008)]," Phys. Fluids **21**, 019902 (2009).
[9] C. B. da Silva, "The behavior of subgrid-scale models near the turbulent/nonturbulent interface in jets," Phys. Fluids **21**, 081702 (2009).
[10] G. Hauët, C. B. da Silva, and J. C. F. Pereira, "The effect of subgrid-scale models on the near wall vortices: A priori tests," Phys. Fluids **19**, 051702 (2007).
[11] S. Stanley, S. Sarkar, and J. P. Mellado, "A study of the flowfield evolution and mixing in a planar turbulent jet using direct numerical simulation," J. Fluid Mech. **450**, 377 (2002).
[12] B. Perot and P. Moin, "Shear-free turbulent boundary layers. Part 1. Physical insights into near-wall turbulence," J. Fluid Mech. **295**, 199 (1995).
[13] O. M. Phillips, "The irrotational motion outside a free turbulent boundary," Proc. Cambridge Philos. Soc. **51**, 220 (1955).
[14] J. Jiménez and A. Wray, "On the characteristics of vortex filaments in isotropic turbulence," J. Fluid Mech. **373**, 255 (1998).
[15] J. C. R. Hunt, I. Eames, J. Westerweel, P. A. Davidson, S. Voropayev, J. Fernando, and M. Braza, "Thin shear layers—The key to turbulence structure," J. Hydro-environment Res. **4**, 75 (2010).
[16] A. I. Ruban and K. N. Vonatsus, "Discontinuous solutions of the boundary-layer equations," J. Fluid Mech. **614**, 407 (2008).